LETTER

doi:10.1038/nature13857

Recent Northern Hemisphere stratospheric HCl increase due to atmospheric circulation changes

E. Mahieu[1], M. P. Chipperfield[2], J. Notholt[3], T. Reddmann[4], J. Anderson[5], P. F. Bernath[6,7,8], T. Blumenstock[4], M. T. Coffey[9], S. S. Dhomse[2], W. Feng[2], B. Franco[1], L. Froidevaux[10], D. W. T. Griffith[11], J. W. Hannigan[9], F. Hase[4], R. Hossaini[2], N. B. Jones[11], I. Morino[12], I. Murata[13], H. Nakajima[12], M. Palm[3], C. Paton-Walsh[11], J. M. Russell III[5], M. Schneider[4], C. Servais[1], D. Smale[14] & K. A. Walker[8,15]

The abundance of chlorine in the Earth's atmosphere increased considerably during the 1970s to 1990s, following large emissions of anthropogenic long-lived chlorine-containing source gases, notably the chlorofluorocarbons. The chemical inertness of chlorofluorocarbons allows their transport and mixing throughout the troposphere on a global scale[1], before they reach the stratosphere where they release chlorine atoms that cause ozone depletion[2]. The large ozone loss over Antarctica[3] was the key observation that stimulated the definition and signing in 1987 of the Montreal Protocol, an international treaty establishing a schedule to reduce the production of the major chlorine- and bromine-containing halocarbons. Owing to its implementation, the near-surface total chlorine concentration showed a maximum in 1993, followed by a decrease of half a per cent to one per cent per year[4], in line with expectations. Remote-sensing data have revealed a peak in stratospheric chlorine after 1996[5], then a decrease of close to one per cent per year[6,7], in agreement with the surface observations of the chlorine source gases and model calculations[7]. Here we present ground-based and satellite data that show a recent and significant increase, at the 2σ level, in hydrogen chloride (HCl), the main stratospheric chlorine reservoir, starting around 2007 in the lower stratosphere of the Northern Hemisphere, in contrast with the ongoing monotonic decrease of near-surface source gases. Using model simulations, we attribute this trend anomaly to a slowdown in the Northern Hemisphere atmospheric circulation, occurring over several consecutive years, transporting more aged air to the lower stratosphere, and characterized by a larger relative conversion of source gases to HCl. This short-term dynamical variability will also affect other stratospheric tracers and needs to be accounted for when studying the evolution of the stratospheric ozone layer.

Decomposition of chlorine-containing source gases in the stratosphere produces HCl, the largest reservoir of chlorine[8,9]. Here we investigate recent trends in atmospheric HCl with observations from eight Network for the Detection of Atmospheric Composition Change (NDACC; http://www.ndacc.org) ground-based stations located between 79° N and 45° S and operating Fourier Transform InfraRed (FTIR) instruments. Figure 1a shows the HCl total columns for Jungfraujoch (47° N; red squares) together with the evolution of the total tropospheric chlorine (blue curve) over the past three decades. Figure 1b–d focuses on the recent HCl changes above Ny-Ålesund (79° N) and two mid-latitude stations, Jungfraujoch (zoom of Fig. 1a) and Lauder (45° S).

At the Southern Hemisphere station we find a continuous decrease of HCl since 2001, but both Northern Hemisphere sites show an overall HCl decline, more rapid around 2004, followed by an increase from 2007 onwards. To quantify the column changes at all sites, we used a bootstrap resampling statistical tool[10] involving a linear component and accounting for the strong seasonal modulations present in the data sets. Figure 2 displays, for the eight NDACC sites, the relative annual HCl rates of change for the 1997–2007 and 2007–2011 time periods, using either the 1997.0 or 2007.0 computed column as reference. For the 1997–2007 time interval, we determine consistent and significant HCl decreases at all Northern Hemisphere sites, with mean relative changes ranging from −0.7 to −1.5 per cent per year. In the Southern Hemisphere, column changes are not significant at the 2σ level. For 2007–2011, mean relative column growths of 1.1–3.4 per cent per year are derived for all Northern Hemisphere sites while negative or undefined rates are observed for Wollongong and Lauder in the Southern Hemisphere.

To corroborate these findings with independent data, and to get information on the altitude range where these changes occur, we included the GOZCARDS[11] satellite data set (Global OZone Chemistry And Related Data sets for the Stratosphere version 1.01), which merges observations by the HALOE[12] (HALogen Occultation Experiment version 19), ACE-FTS[13] (Atmospheric Chemistry Experiment-Fourier Transform Spectrometer version 2.2) and Aura/MLS[14] (Microwave Limb Sounder version 3.3) instruments. Partial columns were computed between 100 hPa and 10 hPa, considering the zonal monthly mean mixing ratio time series available for the whole time interval in the 70°–80° N, 60°–70° N, 40°–50° N, 30°–40° N, 20°–30° N, 30°–40° S and 40°–50° S latitudinal bands. These partial columns typically span altitudes of 16–31 km, that is, the region with maximum HCl concentration and in which the FTIR measurements are most sensitive[5].

Corresponding rates of change are also displayed in Fig. 2. For 1997–2007, there is excellent agreement in the Northern Hemisphere between the satellite and the six NDACC-FTIR trends determined above. In the Southern Hemisphere, GOZCARDS reveals statistically significant decreases of HCl at the 2σ level, while the FTIR time series suggest stable columns at the same level of confidence. For 2007–2011, the ACE-FTS and Aura/MLS merged data confirm the upward FTIR trends in the Northern Hemisphere. Figure 3 illustrates this, showing satellite monthly means (red dots) for 30°–60° N and 30°–60° S, at 46 hPa and 7 hPa, together with a linear fit to the data for both time periods. The HCl increase is clearly confined to the Northern Hemisphere lower stratosphere.

Because HCl is the main final product of the decomposition of any chlorine-containing source gases, we need to verify that its rise after 2007 does not result from the substantial contribution of new unknown sources of chlorine whose emissions occur predominantly in the Northern Hemisphere, not monitored by the *in situ* networks, and unregulated by the Montreal Protocol, its Amendments and Adjustments. Indeed, such chlorine-containing source gases have been recently identified[15],

[1]Institute of Astrophysics and Geophysics, University of Liège, Liège 4000, Belgium. [2]National Centre for Atmospheric Science, School of Earth and Environment, University of Leeds, Leeds LS2 9JT, UK. [3]Department of Physics, University of Bremen, Bremen 28334, Germany. [4]Karlsruhe Institute of Technology (KIT), Institute for Meteorology and Climate Research (IMK-ASF), Karlsruhe 76021, Germany. [5]Department of Atmospheric and Planetary Science, Hampton University, Hampton, Virginia 23668, USA. [6]Department of Chemistry and Biochemistry, Old Dominion University, Norfolk, Virginia 23529, USA. [7]Department of Chemistry, University of York, York YO10 5DD, UK. [8]Department of Chemistry, University of Waterloo, Waterloo, Ontario N2L 3G1, Canada. [9]National Center for Atmospheric Research, Boulder, Colorado 80307, USA. [10]Jet Propulsion Laboratory, California Institute of Technology, Pasadena, California 91109, USA. [11]School of Chemistry, University of Wollongong, Wollongong, New South Wales 2522, Australia. [12]National Institute for Environmental Studies (NIES), Tsukuba, Ibaraki 305-8506, Japan. [13]Graduate School of Environmental Studies, Tohoku University, Sendai 980-8578, Japan. [14]National Institute of Water and Atmospheric Research (NIWA), Lauder 9352, New Zealand. [15]Department of Physics, University of Toronto, Toronto, Ontario M5S 1A7, Canada.

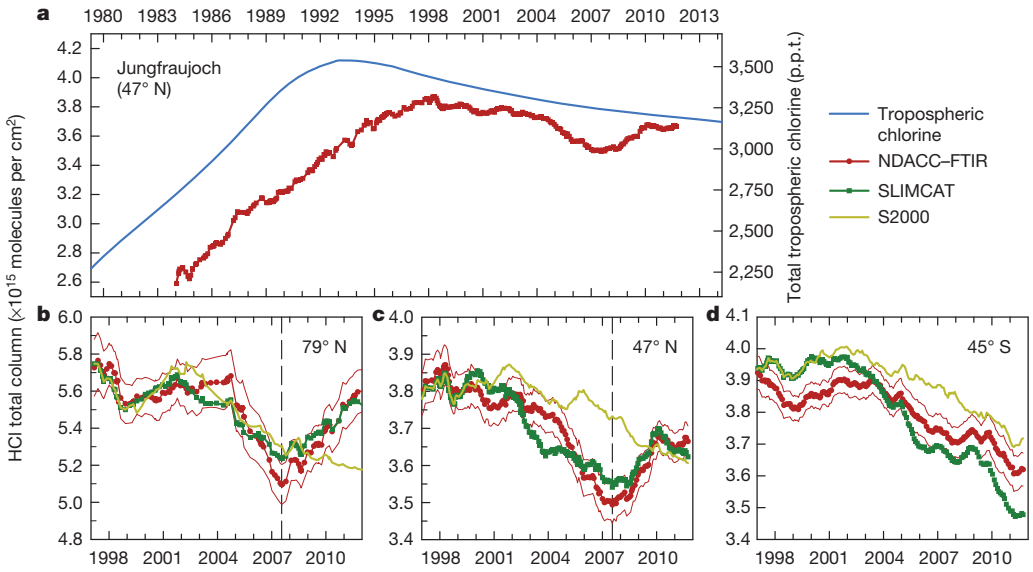

Figure 1 | Evolution of HCl in the Earth's atmosphere. a, The long-term total column time series of HCl at Jungfraujoch (running average with a 3-yr integration length, step of 1 month; in red, left scale) and the global total tropospheric chlorine volume mixing ratio (blue curve, right scale, in parts per trillion, p.p.t). The lower panels display the running average total column time series (1997–2011) of HCl at Ny-Ålesund (**b**), Jungfraujoch (**c**) and Lauder (**d**), derived from the NDACC–FTIR observations, and the standard (green) and S2000 (light green) SLIMCAT simulations. The thin red lines correspond to the ±2 standard error of the mean range. Minimum columns are observed in July 2007 at the Northern Hemisphere sites (dashed lines).

although in that case, their contribution to the HCl upturn can be ruled out by their very low concentrations.

We have used results from two state-of-the-art three-dimensional chemical transport models, SLIMCAT[7] and KASIMA[7], to interpret the recent HCl increase. Both models performed a standard simulation using surface source gas mixing ratios from the WMO A1 (World Meteorological Organisation; 2010) emission scenario[4] and were forced using ERA-Interim meteorological fields[16] from the European Centre for Medium-Range Weather Forecasts (ECMWF). The key results for HCl trends from both models agree. Here we show data from the SLIMCAT runs; corresponding results from KASIMA are shown in Extended Data Figs 1–4. To study the impact of atmospheric dynamics, an additional SLIMCAT run (S2000) used constant 2000 meteorological forcing, from 2000 onwards.

Running averages for both SLIMCAT simulations are reproduced in Fig. 1b–d. For the three sites, run S2000 (light green curve) predicts an overall HCl decrease while the standard run (green squares) reproduces the observed and distinct evolution prevailing in both hemispheres, after correction of a constant low-bias of about 7% in the Northern Hemisphere simulations. The total column changes characterizing the model data sets are displayed in Fig. 2. The model runs predict significant decreases in HCl for the 1997–2007 reference period at all sites and there is an overall agreement within the error bars for the amplitude of the signals between the model and the observations. Regarding the 2007–2011 time period, the SLIMCAT time series are characterized by positive trends from Ny-Ålesund (79° N) to Tsukuba (36° N) and by significant decreases for the Southern Hemisphere stations, but show no change for the near-tropical site of Izana (28° N). The S2000 sensitivity run does not produce the HCl trend reversal and, instead, indicates declines at all sites.

The agreement between measurement and model demonstrates that the HCl increase after 2007 is not caused by new, unidentified chlorine sources, or by underestimates in emissions of known species of chlorine-containing source gases, because these are used as model input. The agreement between model and observation also shows that there is a good understanding of the chemistry which converts source gases to HCl. The difference between the HCl trends forecast by the two SLIMCAT runs—that is, a significant increase for northern high- and mid-latitudes or a constant decrease below 30° N—establishes that changes in the atmospheric circulation cause the recent HCl increase, since only the

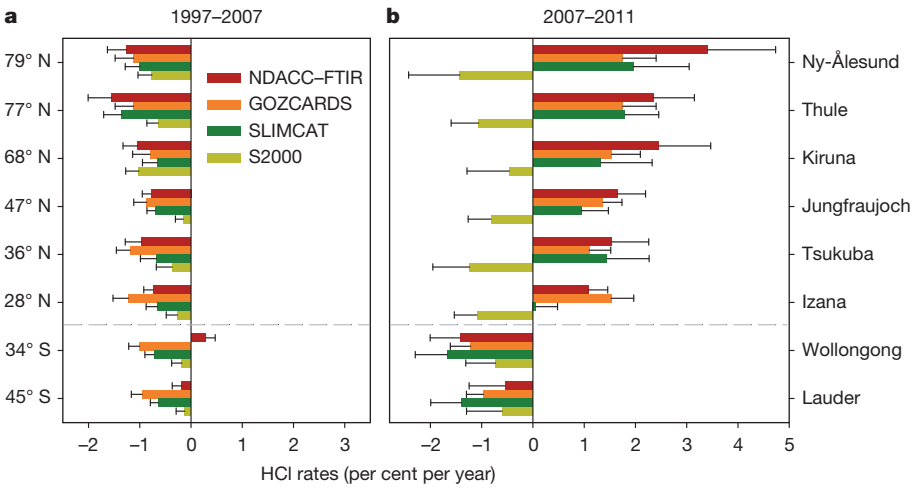

Figure 2 | HCl relative rates of change for eight NDACC sites. a, The rates of change (per cent per year) for the 1997–2007 time period (1999–2007 for Thule and Izana, 1998–2007 for Tsukuba). **b**, As for **a** but for 2007–2011. The rates of change were derived from the FTIR and GOZCARDS observational data sets and from the two SLIMCAT simulated time series (see colour key). The error bars correspond to the 2σ level of uncertainty.

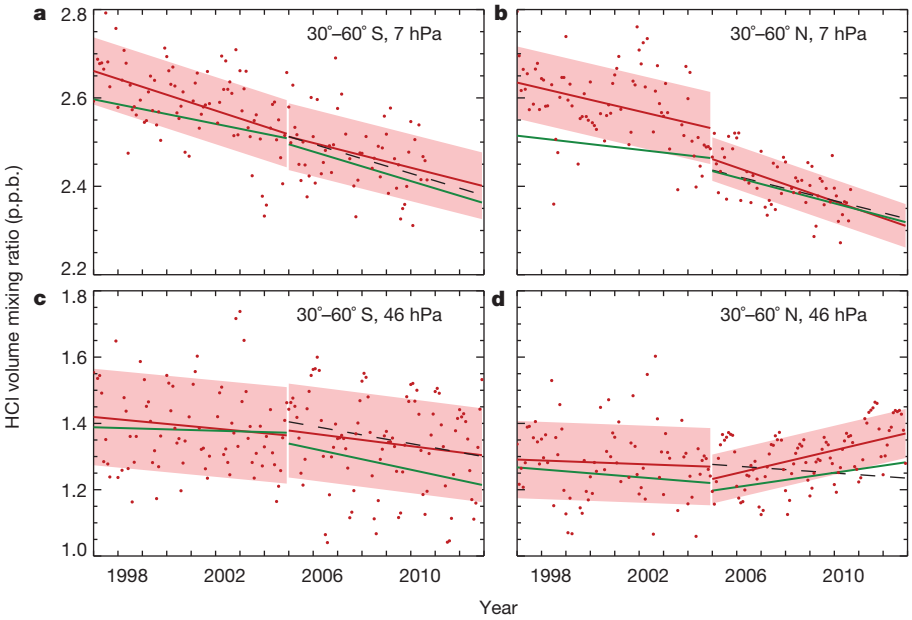

Figure 3 | Evolution of stratospheric HCl from satellite observations. Comparison of merged GOZCARDS satellite HCl observations (by HALOE, ACE-FTS and Aura/MLS) with SLIMCAT model runs for Northern Hemisphere and Southern Hemisphere mid-latitude lower (46 hPa) and upper (7 hPa) stratosphere. GOZCARDS monthly means are shown as red dots. Linear fits to the GOZCARDS data and standard SLIMCAT run are displayed as red and green lines, respectively, for periods before and after 2005. The dashed black line shows fits to the S2000 run, which assumes no change in circulation. An upward trend is observed in the Northern Hemisphere lower stratosphere (**d**) while HCl is decreasing in the southern and northern upper stratosphere (**a**, **b**); volume mixing ratio in parts per billion (p.p.b.).

meteorological fields adopted from 2000 onwards differ between the two runs. To diagnose these circulation changes, we examined age-of-air maps produced by the standard SLIMCAT run. They reveal a slower circulation in the Northern Hemisphere lower stratosphere after 2005–2006, with older air characterized by a larger relative conversion of the chlorine-containing source gases into HCl.

Figure 4b shows the age-of-air change between 2005–2006 and 2010–2011. Air older by up to 0.4 yr is found at altitudes of around 20–25 km in a broad range of Northern Hemisphere latitudes, in a region where the mean age-of-air is typically about 3 yr. There is an obvious correlation with the evolution of the HCl concentrations over the same time period (Fig. 4a), which exhibits a very similar pattern and hemispheric asymmetry. Time series of mean age-of-air near 50 hPa above Ny-Ålesund, Jungfraujoch and Lauder are displayed in Fig. 4c. The 3-yr running means (black curves) indicate a progressive slowdown of the Northern Hemisphere stratospheric circulation after 2005–2006. For Lauder, a fairly constant circulation speedup occurs from 2000 onwards.

These changes are significant at the 2σ level, with Northern Hemisphere air ageing by 3–4 weeks per year after 2005, compared to about 1 week per year before. For Lauder, the mean age-of-air change during the last decade is calculated to be −2 weeks per year. Other important factors, such as the details of specific transport pathways, which lead to a given mean age-of-air, also affect the conversion rate of the source gases to HCl (ref. 17). These pathways are simulated by the model but not revealed by the simple diagnostic of mean age-of-air. The slower Northern Hemisphere circulation occurring over a few years after 2005–2006 seems to contrast with the speedup of the Brewer–Dobson circulation, which is predicted in the very long-term to be a response to climate

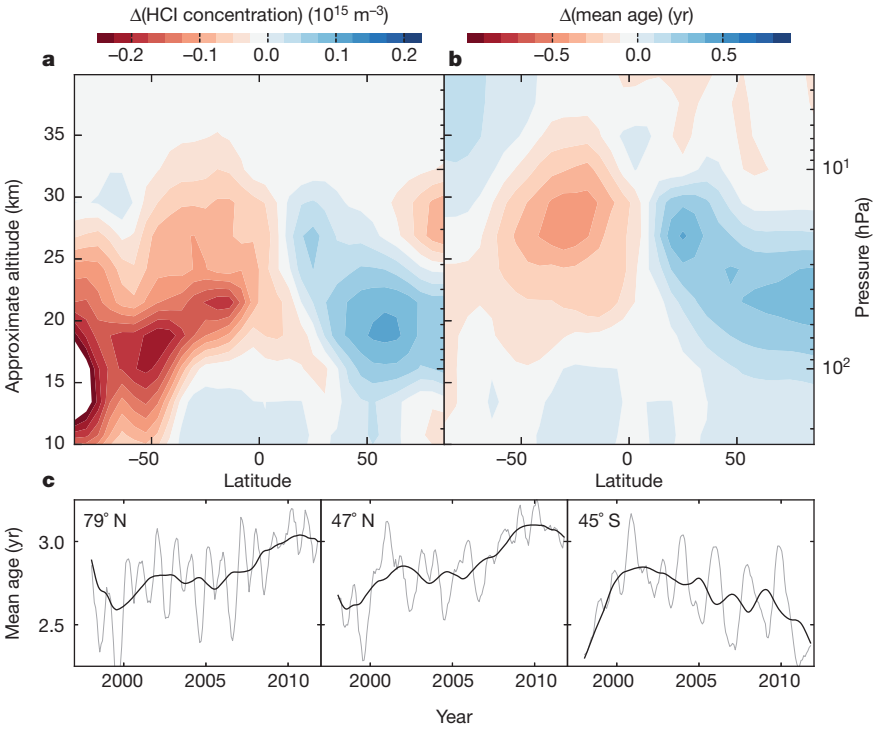

Figure 4 | Spatial distribution of the HCl concentration and age-of-air changes. Mean differences of the HCl concentration (**a**) and age-of-air (**b**) between 2010/2011 and 2005/2006, as a function of altitude and latitude, derived from the standard SLIMCAT simulation. There is a clear asymmetry between the hemispheres, with correlated patterns between age-of-air and HCl, indicating that the HCl changes over that period are consistent with slower/faster circulation in the Northern/Southern Hemisphere. **c**, Running averages of the mean age-of-air at 50 hPa (thick/thin curve, integration length of 36/6 months), at the same sites as Fig. 1 (the time series at 79° N and 45° S have been shifted vertically by −0.75 yr).

change[18,19], but the recent slowdown is probably part of dynamical variability occurring on shorter timescales: it does not imply a change in the general circulation strength. More than year-to-year variability, it is multiyear periods of age-of-air increase or decrease, such as those highlighted in our study or reported recently[20], that will probably complicate the search of a long-term trend in mean circulation.

We have presented observations and simulations of a recent HCl increase in the Northern Hemisphere lower stratosphere. We ascribe it to dynamical variability, occurring on a timescale of a few years, characterized by a persistent slowing of stratospheric circulation after 2005, bringing HCl-enriched air into the Northern Hemisphere lower stratosphere. We find no evidence that unidentified chlorine-containing source gases are responsible for this HCl increase. In the Southern Hemisphere, a fairly constant decrease has been observed over the past ten years. Globally, our ground-based observations indicate a mean HCl decrease of 0.5 per cent per year for 1997–2011, compatible with the 0.5–1 per cent per year range that characterized the post-peak reduction of tropospheric chlorine[4]. Hence, we conclude that the Montreal Protocol is still on track, and is leading to an overall reduction of the stratospheric chlorine loading. However, multiyear variability in the stratospheric circulation and dynamics, as identified here, could lead to further unpredictable increases or redistribution of HCl and other stratospheric tracers. Therefore, such variability and its causes will have to be thoroughly characterized and carefully accounted for when evaluating trends or searching for ozone recovery.

Online Content Methods, along with any additional Extended Data display items and Source Data, are available in the online version of the paper; references unique to these sections appear only in the online paper.

Received 27 March; accepted 10 September 2014.

1. Lovelock, J. E., Maggs, R. J. & Wade, R. J. Halogenated hydrocarbons in and over the Atlantic. *Nature* **241,** 194–196 (1973).
2. Molina, M. J. & Rowland, F. S. Stratospheric sink for chlorofluoromethanes: chlorine atom-catalysed destruction of ozone. *Nature* **249,** 810–812 (1974).
3. Farman, J. C., Gardiner, B. G. & Shanklin, J. D. Large losses of total ozone in Antarctica reveal seasonal ClO_x/NO_x interaction. *Nature* **315,** 207–210 (1985).
4. World Meteorological Organization *Scientific Assessment of Ozone Depletion: 2010* (Report 52, Global Ozone Research and Monitoring Project, WMO, 2011); http://www.wmo.int/pages/prog/arep/gaw/ozone_2010/ozone_asst_report.html.
5. Rinsland, C. P. *et al.* Long-term trends of inorganic chlorine from ground-based infrared solar spectra: past increases and evidence for stabilization. *J. Geophys. Res.* **108** (D8), 27, http://dx.doi.org/10.1029/2002JD003001 (2003).
6. Froidevaux, L. *et al.* Temporal decrease in upper atmospheric chlorine. *Geophys. Res. Lett.* **33,** http://dx.doi.org/10.1029/2006GL027600 (2006).
7. Kohlhepp, R. *et al.* Observed and simulated time evolution of HCl, $ClONO_2$, and HF total column abundances. *Atmos. Chem. Phys.* **12,** 3527–3556 (2012).
8. Zander, R. *et al.* The 1985 chlorine and fluorine inventories in the stratosphere based on ATMOS observations at 30° north latitudes. *J. Atmos. Chem.* **15,** 171–186 (1992).
9. Nassar, R. *et al.* A global inventory of stratospheric chlorine in 2004. *J. Geophys. Res.* **111,** D22312, http://dx.doi.org/10.1029/2006JD007073 (2006).
10. Gardiner, T. *et al.* Trend analysis of greenhouse gases over Europe measured by a network of ground-based remote FTIR instruments. *Atmos. Chem. Phys.* **8,** 6719–6727 (2008).
11. Froidevaux, L. *et al. GOZCARDS Merged Data for Hydrogen Chloride Monthly Zonal Means on a Geodetic Latitude and Pressure Grid* version 1.01, http://dx.doi.org/10.5067/MEASURES/GOZCARDS/DATA3002 (NASA Goddard Earth Science Data and Information Services Center, accessed June 2013).
12. Russell, J. M. III *et al.* The halogen occultation experiment. *J. Geophys. Res.* **98,** 10777–10797 (1993).
13. Bernath, P. F. *et al.* Atmospheric Chemistry Experiment (ACE): mission overview. *Geophys. Res. Lett.* **32,** L15S01, http://dx.doi.org/10.1029/2005GL022386 (2005).
14. Waters, J. W. *et al.* The Earth Observing System Microwave Limb Sounder (EOS MLS) on the Aura satellite. *IEEE Trans. Geosci. Rem. Sens.* **44,** 1075–1092 (2006).
15. Laube, J. C. *et al.* Newly detected ozone-depleting substances in the atmosphere. *Nature Geosci.* **7,** 266–269 (2014).
16. Dee, D. P. *et al.* The ERA-Interim reanalysis: configuration and performance of the data assimilation system. *Q. J. R. Meteorol. Soc.* **137,** 553–597 (2011).
17. Waugh, D. W., Strahan, S. E. & Newman, P. A. Sensitivity of stratospheric inorganic chlorine to differences in transport. *Atmos. Chem. Phys.* **7,** 4935–4941 (2007).
18. Engel, A. *et al.* Age of stratospheric air unchanged within uncertainties over the past 30 years. *Nature Geosci.* **2,** 28–31 (2009).
19. McLandress, C. & Shepherd, T. G. Simulated anthropogenic changes in the Brewer-Dobson circulation, including its extension to high latitude. *J. Clim.* **22,** 1516–1540 (2009).
20. Stiller, G. P. *et al.* Observed temporal evolution of global mean age of stratospheric air for the 2002 to 2010 period. *Atmos. Chem. Phys.* **12,** 3311–3331 (2012).
21. Rothman, L. S. *et al.* The HITRAN 2008 molecular spectroscopic database. *J. Quant. Spec. Radiat. Transf.* **110,** 533–572 (2009).

Acknowledgements The University of Liège contribution was mainly supported by the Belgian Science Policy Office (BELSPO) and the Fonds de la Recherche Scientifique–FNRS, both in Brussels. Additional support was provided by MeteoSwiss (Global Atmospheric Watch) and the Fédération Wallonie–Bruxelles. We thank the International Foundation High Altitude Research Stations Jungfraujoch and Gornergrat (HFSJG, Bern). We thank O. Flock and D. Zander (University of Liège). The SLIMCAT modelling work was supported by the UK Natural Environment Research Council (NCAS and NCEO). The FTIR measurements at Ny-Ålesund, Spitsbergen, are supported by the AWI Bremerhaven. The work from Hampton University was partially funded under the NASA MEASURE's GOZCARDS programme and the National Oceanic and Atmospheric Administration's Educational Partnership Program Cooperative Remote Sensing Science and Technology Center (NOAA EPP CREST). The ACE mission is supported primarily by the Canadian Space Agency. We thank U. Raffalski and P. Voelger for technical support at IRF Kiruna. The National Center for Atmospheric Research is supported by the National Science Foundation. The observation programme at Thule, Greenland, is supported under contract by the National Aeronautics and Space Administration (NASA) and the site is also supported by the NSF Office of Polar Programs. We thank the Danish Meteorological Institute for support at Thule. Work at the Jet Propulsion Laboratory, California Institute of Technology, was performed under contract with NASA; we thank R. Fuller for help in producing the GOZCARDS data set, and work by many ACE-FTS, HALOE and MLS team members who helped to produce data towards the GOZCARDS data set is also acknowledged. We thank O. E. García, E. Sepúlveda, and the State Meteorological Agency (AEMET) of Spain for scientific and technical support at Izana. The Australian Research Council has provided notable support over the years for the NDACC site at Wollongong, most recently as part of project DP110101948. Measurements at Lauder are core funded through New Zealand's Ministry of Business, Innovation and Employment. We are grateful to all colleagues who have contributed to FTIR data acquisition. We thank ECMWF for providing the ERA-Interim reanalyses.

Author Contributions M.P., J.W.H., F.H., E.M., I. Murata, N.B.J., C.P.-W. and D.S. performed the Ny-Ålesund, Thule, Kiruna and Izana, Jungfraujoch, Tsukuba, Wollongong and Lauder retrievals for HCl, respectively. P.F.B. and K.A.W. provided ACE-FTS data; L.F. and J.A. provided the GOZCARDS data set. J.A., P.F.B., L.F., J.M.R. III and K.A.W. provided expertise on satellite data usage. M.P.C., R.H., S.S.D. and W.F. designed and performed the SLIMCAT runs, sensitivity analyses and transport diagnostics. T.R. performed the KASIMA model run and corresponding diagnostics. B.F. and E.M. performed the trend analyses and compiled the results. J.N., M.T.C., T.B., C.S., I. Morino, H.N., M.S., D.W.T.G. and D.S. are responsible for the instrumentation and data acquisition at the NDACC stations. E.M. initiated and coordinated the study. The figures were prepared by E.M. and B.F. (Fig. 1), E.M. (Fig. 2), R.H. and M.P.C. (Fig. 3) and T.R. (Fig. 4). E.M., M.P.C. and J.N. wrote the manuscript. Together with T.R., they revised it and included the comments from the co-authors.

Author Information NDACC data are publicly available at ftp://ftp.cpc.ncep.noaa.gov/ndacc/station/ and GOZCARDS data are publicly available at http://measures.gsfc.nasa.gov/opendap/GOZCARDS/. Reprints and permissions information is available at www.nature.com/reprints. The authors declare no competing financial interests. Readers are welcome to comment on the online version of the paper. Correspondence and requests for materials should be addressed to E.M. (emmanuel.mahieu@ulg.ac.be).

METHODS

The ground-based observations were performed at the NDACC sites by solar absorption spectrometry in the infrared spectral region, using FTIR high-resolution instruments. Observations are recorded under clear sky conditions year-round, except at Ny-Ålesund and Thule, where the polar night prevents measurements between about October and February. The HCl total columns were retrieved with the SFIT-2, SFIT-4 or PROFFIT algorithm in narrow spectral ranges encompassing isolated lines of HCl[5,7], generally assuming pressure-temperature profiles provided by the National Centers for Environmental Prediction (NCEP). The GOZCARDS[11] data set for HCl includes zonal average monthly mean time series of stratospheric mixing ratio profiles merging individual measurements from the HALOE (1991–2005), ACE-FTS (2004 onward) and Aura MLS (2004 onward) satellite-borne instruments. Line parameters from recent HITRAN databases[21] were adopted in the spectrometric analyses. We used the SLIMCAT and KASIMA models[7] to support our investigations. Both used ERA-Interim analyses provided by ECMWF[16], and they provided consistent results for the HCl trends, giving confidence in their robustness. The models contain detailed treatments of stratospheric chemistry and have been extensively used for studies of stratospheric ozone[7]. Stratospheric age-of-air was diagnosed in the model runs using an idealized tracer with a linearly increasing tropospheric mixing ratio. For the S2000 SLIMCAT simulation, 6-hourly winds of 2000 were used every year from 2000 onwards. The trend determinations were performed with a bootstrap resampling statistical tool[10], considering all available daily or monthly means (excluding the winter months for the very high-latitude sites) while the model data sets were limited to days with available FTIR measurements. We studied the impact of the FTIR sampling using the bootstrap algorithm, and found no statistically significant impact on the calculated trends.

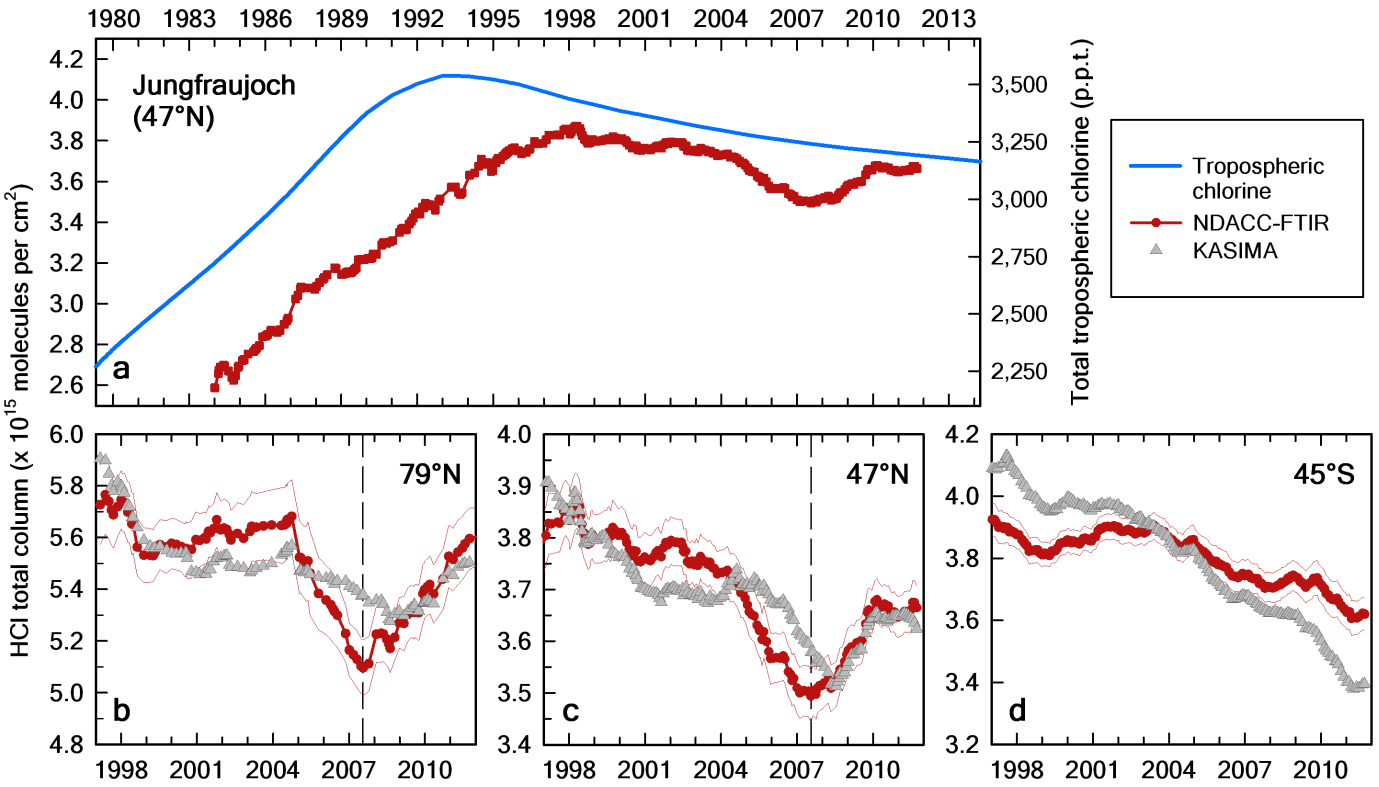

Extended Data Figure 1 | Evolution of HCl in the Earth's atmosphere and comparison with KASIMA model results. a, The long-term total column time series of HCl at Jungfraujoch (running average with a 3-yr integration length, step of 1 month; in red, left scale, in molecules per cm^2) and the global total tropospheric chlorine volume mixing ratio (blue curve, right scale). Lower panels display the running average total column time series (1997–2011) of HCl at Ny-Ålesund (**b**), Jungfraujoch (**c**) and Lauder (**d**), derived from the NDACC–FTIR observations and from the KASIMA run (grey). The thin red lines correspond to the ±2 standard error of the mean range. The vertical dashed lines identify the occurrence of the minimum total columns at the Northern Hemisphere sites, in July 2007.

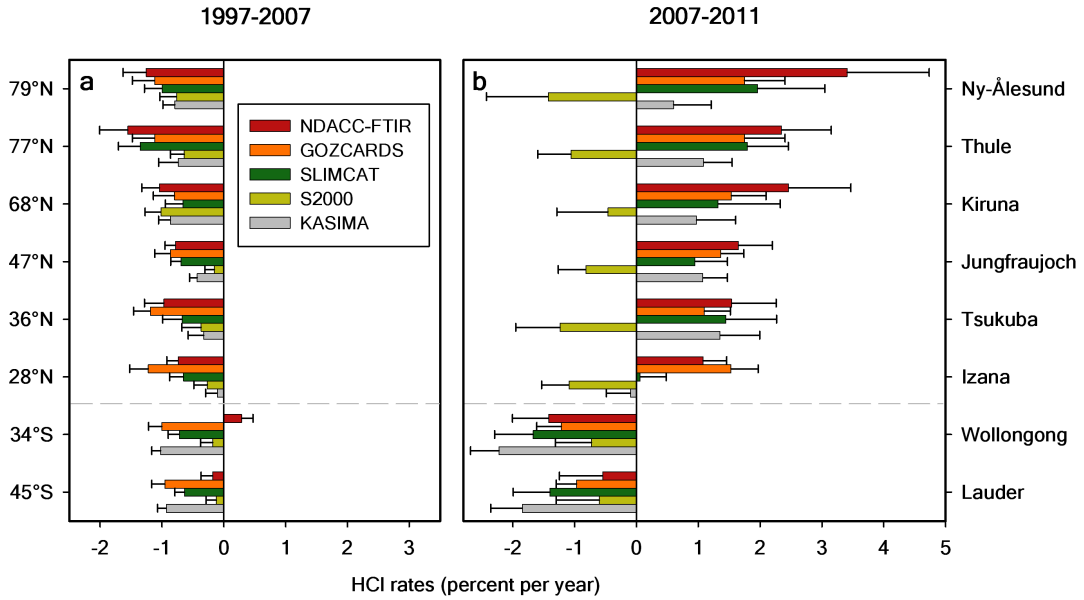

Extended Data Figure 2 | HCl relative rates of change at eight NDACC sites. **a** and **b** provide the rates of change (per cent per year) for the 1997–2007 (1999–2007 for Thule and Izana, 1998–2007 for Tsukuba) and 2007–2011 time periods, respectively. They were derived from the FTIR and GOZCARDS observational data sets and from the SLIMCAT and KASIMA simulated time series (see colour key). The error bars correspond to the 2σ level of uncertainty.

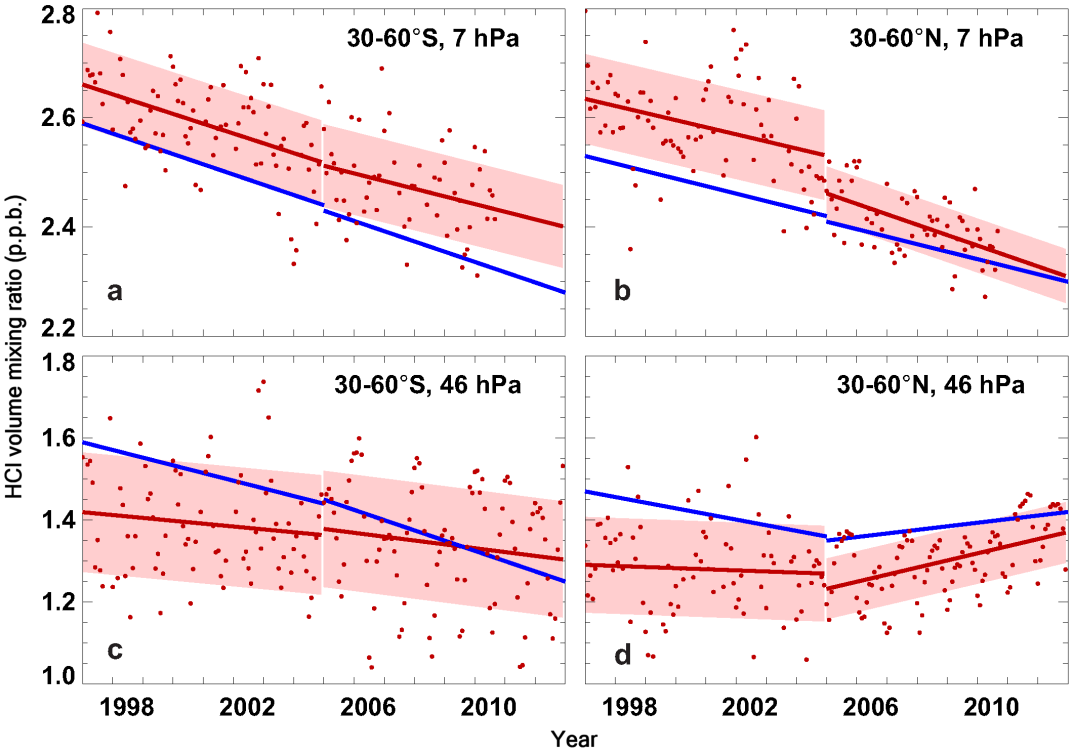

Extended Data Figure 3 | Evolution of stratospheric HCl from satellite observations. Comparison of merged GOZCARDS satellite HCl observations (by HALOE, ACE-FTS and Aura/MLS) with KASIMA model results for Northern and Southern Hemisphere mid-latitude lower (46 hPa) and upper (7 hPa) stratosphere. GOZCARDS monthly mean observations are shown as red dots. Linear fits to the GOZCARDS data and the KASIMA run are displayed as red and blue lines, respectively, for periods before and after 2005. An upward trend is observed and modelled in the Northern Hemisphere lower stratosphere (**d**) while HCl is decreasing in the southern and northern upper stratosphere (**a**, **b**); volume mixing ratio in parts per billion.

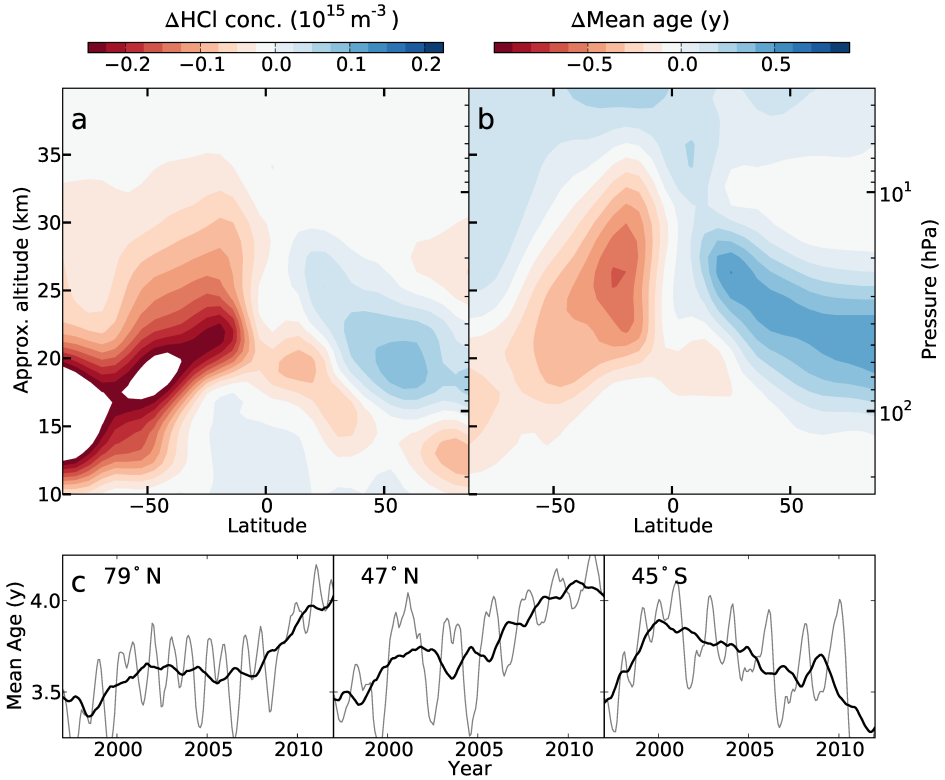

Extended Data Figure 4 | Spatial distribution of the HCl concentration and age-of-air changes. Mean differences of the HCl concentration (**a**) and age-of-air (**b**) between 2010/11 and 2005/06, as a function of altitude and latitude, derived from the KASIMA model simulation. **c**, Running averages of the mean age-of-air at 50 hPa (thick/thin curve, integration length of 36/6 months), at the same sites as in Fig. 1 (time series at 79° N/45° S have been shifted vertically by −0.75/−0.50 yr). Comparison with age-of-air time series derived from SLIMCAT (see Fig. 4c) indicates that KASIMA provides higher absolute values of mean age-of-air. Note that the upper boundary of KASIMA is at 120 km, yielding higher mean ages, compared to SLIMCAT (upper boundary 60 km).